

On the Influence of Wind Turbines on Radars

Emmanuel Van Lil¹, Dave Trappeniers², Antoine Van de Capelle³

¹ K.U.Leuven, div. ESAT-Telemic, Kasteelpark Arenberg, 10 – box 2444, B-3001 Heverlee,
E-mail: Emmanuel.VanLil@esat.kuleuven.be

² As ¹ above, but E-mail: Dave.Trappeniers@esat.kuleuven.be

³ As ¹ above, but E-mail: Antoine.VandeCapelle@esat.kuleuven.be

Abstract

Previous studies have been focusing on the influence of moving objects like wind turbines on aeronautical and maritime radars, working usually respectively in the L/S band and in the X-band. Here, those results will be summarized for a special kind of radars, usually working in the C band, namely meteorological radars. We have used both UTD methods as well as simplified methods to quantize the effects. Indeed, not many moment method solvers have the possibility to deal with moving objects (creating Doppler shifts), but with UTD it is within easy reach of the modern computers. However, for some particular applications, the procedures can be simplified to quantize efficiently the near-fields around moving objects. After a description of the general phenomena, two simplified methods will be compared. The first consists in a Physical Optics based method, and the second does make use of the flat wedge approximation.

1. Introduction

The main effects of wind turbines on radars have been described in previous papers [1], [2]. They include shadowing by the larger parts and generation of false echoes. For meteorological radars those effects are now distributed in nature, since a cloud is not a well delimited target like a ship or a plane. The second most important difference is that Doppler measurements are used by meteorologists to determine wind speeds inside the clouds. Aeronautical radars did already have some Doppler measurements, but more specially to eliminate (static) clutter from the radar screens (MTI Moving Target Indicator). In the meantime a lot of European agencies are trying to generate coherent standards for the whole of Europe. One example is the French ANFR (Agence Nationale pour les FRéquences) [3]. Even if more elaborate, full 3D UTD, methods have been developed [2], it is sometimes useful to have a fast but still accurate idea of the effects of moving objects. We will use some approximations to allow a fast but still accurate computation of effects of the moving blades. The first approximation to be done is to simplify the shape of the moving objects. One shape that is suited to the description of the blade of a wind turbine is the cylindrical shape. On the other hand, it is very difficult to obtain the real data on the blade shape, since this is usually considered by most manufacturers as a “fabrication secret”. It has the advantage that the monostatic radar cross-section of a cylinder is known in an analytical way, like those of many other simple shapes. It has to be noted that those analytical formulas are known only for the far-field case. So, they will have to be adapted to deal with the near-field case. Another possibility consists in just using the flat edge diffraction formulas. Further all multiple effects (multiple reflections/diffractions) will be neglected, as well as corner diffractions.

2. Shadowing

Nowadays rain radars do appear on the web in nearly real time (a delay of 15' being common). The peak in the cross-section of the shadowing effect computed with EPICS is due to the blades (Fig. 1). All the classical effects like shadowing can be seen as before (Fig. 2). The deep shadowing zone extends more in the meteorological case than the aeronautical case, but less than the maritime case, due to the C-band frequency of usually around 5.6 GHz, between the maritime X-band and aeronautical S or L bands. All figures here assume vertical polarization.

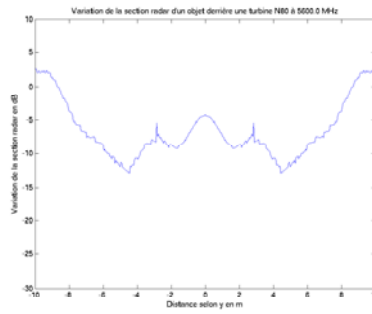


Fig. 1: cross-section of the variation of the RCS behind a metallic N80 turbine (13 km from the radar; the cross-section is at -15 km).

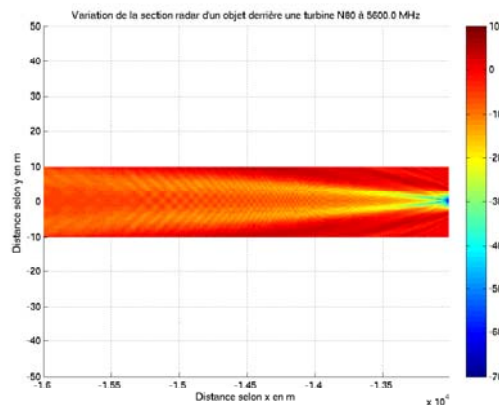


Fig. 2: variation of the RCS of an object behind an N80 turbine in metal for a C band meteorological radar.

How it appears on the radar screens is clearly visible. Indeed, for the meteorological radar of the Netherlands from the “KNMI” in “De Bilt”, close to the city of Utrecht, this can be clearly seen on the cloud picture (Fig. 3). The left part is the background, and the right part is the cloud radar picture. This image has been downloaded from the site www.weerradar.nl. The North is not towards the top of the page, but slightly inclined (3,5° counter clockwise). White stripes mark a fictitious decrease of the rain echoes. This is due to obstructions like large buildings, but could be corrected for with appropriate propagation software. The stability of the stripes is clearly illustrated in the original illustration which contains the animation of the moving clouds. The origin of this blockage can clearly be seen when looking at the long optical shadows around Utrecht in Google Earth (Fig. 4). Since those buildings are much larger than relatively small wind turbines, their effects are much larger. The tower corresponding with the SSE stripe has a cross-section perpendicular to the radar of about 71 m (compare this with a turbine of about 5 m diameter at the lowest part above the local ground).

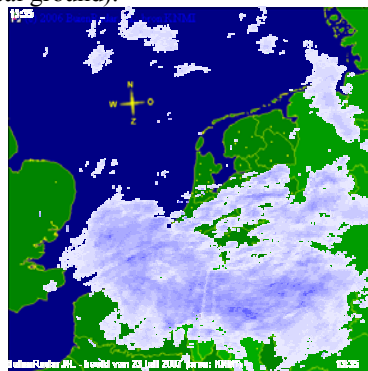


Fig. 3: rain over the Benelux by the Dutch weather radar during the thunderstorms of 23 July 2007.

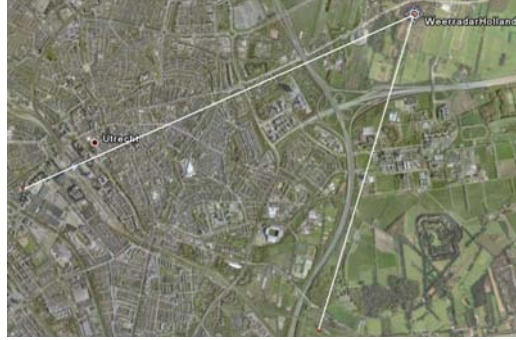


Fig. 4: principal obstructions influencing the good working of the Dutch KNMI weather radar.

3. False Echoes

Since the cloud is distributed, the area is limited by the spatial extend of the radar pulse. Furthermore, one droplet of rain with radius a has a monostatic RCS smaller than (this assumes full illumination of the droplet):

$$\frac{\sigma_m}{\pi a^2} = \frac{2}{(2\beta a)^2} \{1 - \cos(4\beta a) + 4(\beta a)^2 [1 + \cos(4\beta a)] - 4\beta a \sin(4\beta a)\} \left| \frac{\varepsilon - 1}{\varepsilon + 2} \right|^2 \quad (1)$$

For small a , this becomes [5]: $\sigma_m = \pi a^2 (\beta a)^4 64/9 \left| \frac{\varepsilon - 1}{\varepsilon + 2} \right|^2$; $\beta = \frac{2\pi}{\lambda}$. The permittivity ε of water is about 15 at 5.6 GHZ (depending on the temperature and the degree of impurities this might vary between 10 and 20). The received signal from one droplet is hence:

$$P_{fs} = \frac{P_t G_t G_r \sigma_m \lambda^2}{(4\pi)^3 R^4} \quad (2)$$

Note that this formula includes the permittivity. Indeed, the RCS depends also of the type of precipitation (a snowflake has a smaller RCS than a water droplet of the same size). Since a radar does not have the resolution of a water droplet, the radars detects a mean over a given volume or:

$$P_{fs} = \frac{P_t G_t G_r \lambda^2}{(4\pi)^3 R^4} \int_V \sigma'_m(\vec{r}) dV \quad (3)$$

where $\sigma'_m(\vec{r})$ is the product of the raindrop density with their RCS. Meteorologists prefer to express this quantity in function of the distribution of the raindrop size. This distribution is usually an exponential, with a maximal diameter. Indeed, a too big droplet breaks down into smaller ones. The precipitations (in mm/h) being proportional to:

$$R = \int_0^{D_{max}} N_0 e^{-\Delta D/D_0} (\pi D^3 / 6) v(D) dD \quad (4)$$

where v is the falling speed of a droplet of diameter D . This allows the meteorologist to connect this rain rate R to the radar return P_{fs} by a simple equation of the type $P_{fs} = a R^b$. The coefficients of this equation can be found in ITU-R recommendation P.838 to compute a wave attenuation for different polarizations and frequencies.

In this study circular droplets have been assumed. The volume over which we have to integrate is $V = \pi R^2 \Delta \theta_{3db}^2 c \tau / 4$, where $\Delta \theta$ is the beamwidth and τ the width of the radar pulse (twice the resolution). For a distance of 13 km and a beamwidth of 1° this corresponds with about 20000000 m³ of clouds. With an intensity of 64 dBz (or an extremely heavy rain of 364.6 mm/h), this leads us to an RCS of 2281 m². Note that in the classical formulas for false echoes, σ_{BA} and σ_{MA} are proportional with the distance R_{AR}^2 .

This leads to false echo zones that are smaller closer to the radar and larger away from the radar in comparison with the fixed target case. So, they never coincide with the radar location. Again, on days of heavy rain, this can be seen on a poorly located meteorological radar (Fig. 5).

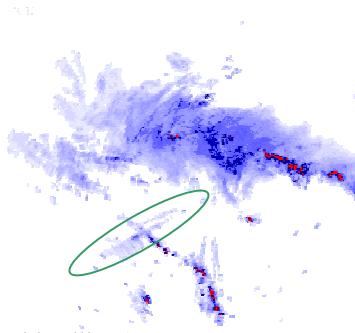


Fig. 5: false echoes on a weather radar (inside ellipse)

4 Doppler effects

So, the object is limited to its far-field size by limiting it to a size equal to $D = \sqrt{(\lambda R)/2}$, being the inverse of the phase far-field distance $R \leq 2D^2 / \lambda$. Then it is enough to limit its size to the coherent part of the blade and use this size with the radar equation and the far-field RCS formulas. It should be noted that this coherent part will be even less if the surface seen from the radar is convex, but might be larger due to the focusing effect if the surface is concave. Measured data can be found on public domain reports [5], Fig. 6, left part. Using this RCS simplification, we can simulate this effect. Depending on the orientation of the turbine, we can obtain similar results. We have verified that the amplitude of the return is similar for the case of a flat wedge diffraction.

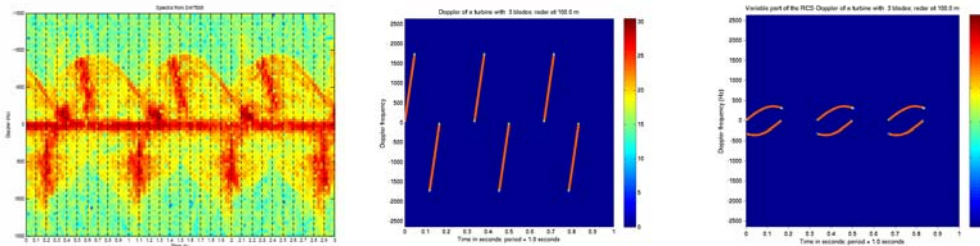


Fig. 6: Measured (left) and simulated Doppler returns (0° and 70° rotated gondola; the radar is 100 m from turbine)

5. Conclusions

The study of the distance requirements of meteorological radars is in many points different from the previous studies (aeronautical and maritime). It is amazing to note how a few simple formulas can explain phenomena, which cannot yet be computed by the most complex commercial moment method solvers.

6. Acknowledgments

We are indebted to the different regulatory agencies like Belgocontrol, the Schelderadarketen as well as the air and sea components of the Belgian armed forces for their open-minded collaboration. Also the main contractors like Suez, Nuon, Total and C-power as well as many less known companies for awarding us the possibility to investigate those effects.

7. References

1. D. Trappeniers, E. Van Lil and A. Van de Capelle, "Effects of Wind Turbines on Aeronautical Radars", COST273, Towards Mobile Broadband Multimedia Networks, Athens, Greece, TD(04)050.1-11, 26-28 Jan. 2004
2. D. Trappeniers, E. Van Lil and A. Van de Capelle, "Effects of objects with moving parts like wind turbines on maritime RF safety and navigation systems", European Conference on Antennas and Propagation (EuCAP) 2006, Nice, France, pp1-5, 6-10 Nov. 2006
3. ANFR, Rapport CCE5 n° 1, "Perturbations du fonctionnement des radars météorologiques par les éoliennes", 2005 (<http://www.anfr.fr>)
4. D.K. Barton, "Modern Radar System Analysis", Artech House, 1988
5. G. Poupart, "Wind Farms Impact on Radar Aviation Interests - Final Report", W/14/00614/00/REP, Qinetiq; can be downloaded from <http://www.bwea.com/aviation/radar.html>